Proceedings of 20th International Congress on Acoustics, ICA 2010

23-27 August 2010, Sydney, Australia

The force transmissibility of a floating slab track

Dominik Duschlbauer (1)

(1) AECOM, Sydney, Australia

PACS: 43.40.At, 43.40.Tm

ABSTRACT

The force transmissibility of a track isolation system is the ratio of the force transmitted to the track bed over the force applied at the railheads. This paper focuses on the force transmissibility of a double-tie or 'mini-slab' floating slab track installation. The power spectral densities of the forces transferred to ground due to 'white noise' force sources at the rail heads are calculated. Analytical models and the Finite Element (FE) method are used to analyse a floating slab track supported on a rigid foundation. The effect of rail fastener stiffness is discussed. The influence of the flexibility of the floating slabs and the effects of a non-rigid foundation on the force transmissibility is investigated within the framework of the FE method.

INTRODUCTION

Joining structural subsystems with resilient elements provides an opportunity to design a system's vibration transmission characteristics. Adequately designed, resilient interfaces reduce the transmitted forces to a fraction of the levels associated with rigid interfaces.

The resilience in tracksupport was traditionally provided by ballast. Increasingly restrictive noise and vibration requirements and lower life-cycle costs resulted in a transition to ballastless, vibration isolated trackforms.

In this paper the vibration isolation performance of a floating slab track (FST) is investigated. The modelled FST is based on the installation at Chatswood Transport Interchange in Sydney, Australia. This interchange features an elevated rail platform and a platform for future apartment towers to be constructed over the rail line within an integrated building structure. In addition to the FST vibration control measures include high compliance rail fasteners, a low mobility deck and stiff columns. Background and technical information can be found in Refs. 3 and 4.

Rigid floating slabs on a rigid deck are investigated first. One and two degree of freedom lumped mass models and Finite Element (FE) models are used to highlight characteristic dynamic features of FST isolation. Subsequently, the impact of flexibility on the vibration isolation performance is studied. The effects of flexible slabs and flexible FST support structures are studied separately.

METHODOLOGY

In general the modelled domain comprises the FST (inclusive the unsprung mass of one bogie), the train deck and deck support. The deck support structure is assumed to be on rigid ground (Figure 1).

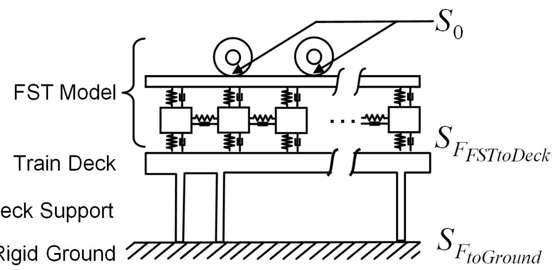

Figure 1. Schematic diagram showing the FST (including unsprung mass) and the supporting train deck structure.

Linear random vibration theory [Ref. 1] was used to calculate force transmissibilities. Uncorrelated, 'white noise' random forces in vertical direction of unit power spectral density $S_F(f)=S_0$ were applied at the element(s) representative of the wheel/rail interface at model level. Upper case S is used to signify that a variable is a power spectral density (PSD).

The stationary random response was calculated and the PSDs of the vertical forces transferred to ground were computed and converted to one-third octave band forces.

The force transmissibility was calculated for each one-third octave band as the ratio of the force transmitted to ground, $F_{toGround}$, over the applied force, F_0. Force transmissibilities are presented in terms of decibels (Eq. 1).

$$T_{dB} = 20 \times \log_{10}\left(F_{toGround} / F_0\right) \qquad \text{(Eq. 1)}$$

Results are presented from the 3.15 Hz to 315 Hz one-third octave bands and the underlying narrowband PSDs were calculated to at least 356 Hz.

A positive transmissibility indicates amplification, i.e. the force transferred to ground is greater than the force applied. Conversely, a negative transmissibility indicates attenuation and the force transferred to ground is less than the force applied.

In literature the term ‘insertion gain’ (or loss) is commonly used to compare the performance of one trackform relative to a stiffer and (typically) continuously supported reference track (Ref. [8]). The calculated force transmissibilities cannot be compared with insertion gains since the underlying reference track is infinitely stiff.

The framework of random vibration assumes that the excited system has reached stationary conditions. A rolling wheel, however, represents a non-stationary source. For example a 10 Hz single degree of freedom system damped at 5% critical damping will require at least 5 seconds to approach its stationary limit [Ref. 1]. Furthermore, the wheel/rail interface forces are of random, impact-like nature rather than of continuous steady-state nature [Ref. 6]. These effects are not accounted for in the chosen framework and would need to be considered separately depending on the problem setup.

The models account for the effects of the unsprung mass which is critical in determining force transmissibilities. Axles and wheels are implemented as rigid bodies. These assumptions start to loose validity at frequencies above 250-300 Hz due to radial wheel modes [Ref. 5].

ANALYTICAL MODELS

Two lumped mass models utilizing discrete springs and dampers are employed (Figure 2). An 11.5 Hz one degree of freedom system (1DOF) and a two degree of freedom system (2DOF) tuned to 11.5 Hz (fundamental vertical FST mode) and 38 Hz (fundamental vertical rail mode with unsprung mass).

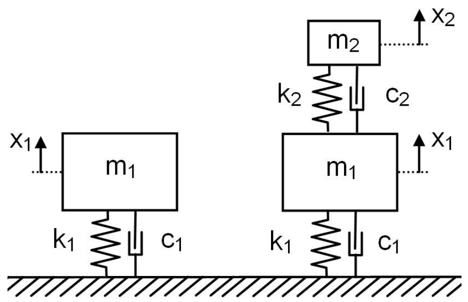

Figure 2. Single and two degree of freedom models

The response PSD of the displacement of mass m_1, S_{x_1}, due to a force spectral density, S_0, was calculated from Eq. 2. In the 1DOF model S_0 is applied at m_1, and in the 2DOF model S_0 is applied at m_2. The *gain function* |H| is the modulus of the ratio of the complex displacement response of m_1 divided by the complex forcing function (see [Refs. 1, 2]).

$$S_{x_1}(f) = \left|H(f)\right|^2 \times S_0 \quad \text{(Eq. 2)}$$

The PSDs of the spring force, S_{F_k}, and damper force, S_{F_c}, to ground was calculated from Eqs. 3 and 4.

$$S_{F_k}(f) = k_1^2 \times S_{x_1}(f) \quad \text{(Eq. 3)}$$

$$S_{F_c}(f) = c_1^2 \times (2 \times \pi \times f)^2 \times S_{x_1}(f) \quad \text{(Eq. 4)}$$

The total one-third octave force transferred to the ground, $F_{toGround}$, was calculated from $S_{toGround}$, which is the sum of the PSDs of the spring and damper forces (Eq. 5). The spring and damper are in parallel and can be thought of as a ‘viscously damped spring’. Adding damping and spring force *spectra* (as opposed to PSDs) requires Pythagoras’ rule.

$$S_{toGround} = S_{F_k} + S_{F_c} \quad \text{(Eq. 5)}$$

In Eqs. 3 and 4, k_1 and c_1 are the spring and damping constants linking m_1 to a rigid foundation. The parameters used for the two lumped mass models are presented in Table 1 and correspond to 5% critical damping.

Table 1. System parameters for lumped mass models.

	1DOF	2DOF	
m_1	11570	8600	kg
m_2	-	2970	kg
k_1	60.4	62.7	MN/m
k_2	-	120	MN/m
c_1	83.6	73.4	kNs/m
c_2	-	49.0	kNs/m

FINITE ELEMENT MODELS

The Finite Element (FE) models were built and solved in Abaqus 6.9 [Ref. 7].

FST Model

The FST model was based on the model described in Ref. [3]. The number of slabs was increased from 15 to 19 to match the length of the supporting deck.

The rails were attached to the slabs with translational springs with three orthogonal springs with a stiffness of 10 MN/m. The rails were modelled as quadratic Euler-Bernoulli beams.

Two axles (320 kg/axle) and four wheels (440 kg/wheel) at 2.4 meters offset were included. The wheels were modelled as lumped masses and attached to the rigid axles (Figure 3). The translational DOFs of the rail and the wheels/axles were coupled.

A Young's modulus of 30 GPa, Poisson's ratio of 0.25 and a density of 2400 kg/m^3 were adopted for the concrete and the mass per slab was 3200 kg. The slabs were meshed with quadratic solid elements. Depending on the modelling scenario, the slabs were either constrained to rigid bodies or left flexible. Each slab was supported (and connected to the deck) by four main support pads under the slab and four sidepads. All pads are implemented as translational springs. The combined vertical support stiffness of one slab was 20 MN/m.

Train Deck Model

The thickness of the supporting train deck was 1.4 m. Its thickness was reduced to 1.0 m directly under the FST where a trough is formed to accommodate the floating slabs (Figures 3 and 4). The deck sections were vertically offset by 250 mm and the edges were tied by constraint equations ensuring continuity (Figure 4). The deck was meshed with triangular elements using quadratic interpolation functions. The element size was approximately 200 mm, which is sufficient to accurately capture deck deflections up to 700 Hz.

The deck was supported on diameter 500 mm columns arranged in a 8.4x6.75 m grid. The middle row of columns ran directly under the FST (Figure 4). The columns were meshed with quadratic Euler-Bernoulli beams. The top of the columns interfaced with circular regions on the deck and the bases were clamped.

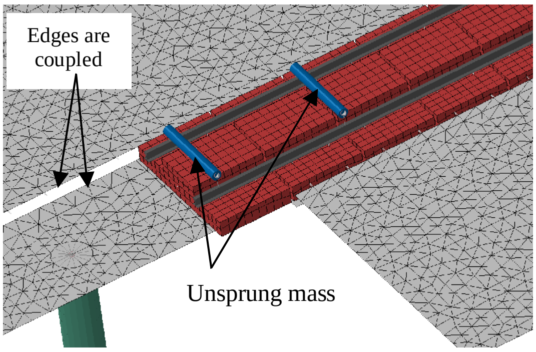

Figure 3. Isoview of the FE model: Axles (blue), rails (dark grey), slabs (red), column (green) and the deck (grey).

The material properties of the deck and columns were the same as those of the slabs. The steel reinforcing in the concrete was not explicitly accounted for in the model.

The deck is free move in vertical direction. Displacement normal to the perimeter in the horizontal direction is restrained.

A total of three different deck and deck support scenarios were considered. Firstly, a rigid train deck on rigid deck supports was considered. This modelling scenario is referred to as 'RD'. In the corresponding FE model, the deck and support columns were removed from the model and the springs supporting the floating slabs were connected directly to ground. Secondly, the effects of a flexible train deck on rigid support points were considered. This assumption was realized by removing the columns from the model and pinning the centre points of the circular deck areas. This modelling scenario is referred to as 'FD(pS)'. And thirdly, a flexible deck on flexible columns was considered (referred to as 'FD(fC)').

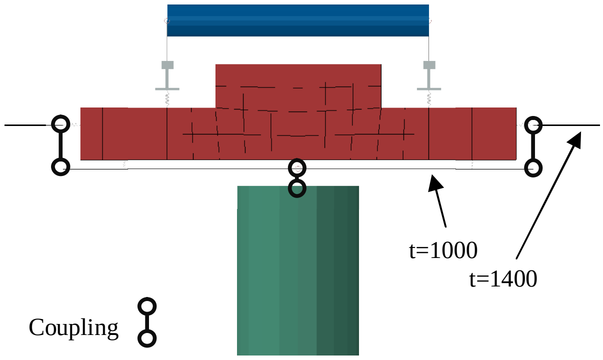

Figure 4. Cross sectional view of the FE model.

Analysis Technique

Random response analyses were used to calculate the stationary response of each model. This analysis type uses mode superposition and was preceded by a mode extraction step in which the modes up to 700 Hz were extracted.

The models were loaded with four *uncorrelated* white noise sources, applied at each wheel/rail contact point in vertical direction. Damping was modelled in terms of fraction of critical damping and 5% critical damping was applied across all frequencies.

In the random response analysis the results variables are expressed as PSD values of nodal and element variables. Due to the implementation of damping in the chosen analysis type only the stiffness contribution of the viscously damped springs, S_{F_k}, was calculated as output. The PSDs of damping forces, S_{F_c}, were estimated from S_{F_k} using Eqs. 3 and 4 and k_1 and c_1 of the 1DOF model (Table 1). The PSD forces transferred to ground were then calculated with Eq. 5 and converted to one-third octave bands, $F_{toGround}$ for each spring/reaction point and subsequently summed.

The method used to model the effects of damping and to evaluate damping forces is a purely mathematical concept. It is an approximate method.

For the calculation of $F_{toGround}$ a total of three cases needed to be considered. For the 'RD'-case (i.e. rigid deck, deck support structure) $F_{toGround}$ was calculated directly from the slab support springs. For the 'FD(fC)'-case (i.e. flexible deck, flexible deck support) $F_{toGround}$ was calculated from the vertical reaction forces at the base of the columns. For the 'FD(pS)'-case (i.e. flexible deck, rigid deck support) $F_{toGround}$ was calculated from the vertical reaction forces of the pinned deck supports.

RESULTS

The abbreviations used to reference the investigated scenarios are listed in Table 2.

Table 2. Model overview.

ID	Description
1DOF	Lumped mass model, 1 degree of freedom
2DOF	Lumped mass model, 2 degrees of freedom
RS-RD	FEM, rigid slabs on a rigid deck
FS-RD	FEM, flexible slabs on a rigid deck
RS-FD(pS)	FEM, rigid slabs on a flexible deck on pinned support points
RS-FD(fC)	FEM, rigid slabs on a flexible deck supported on columns

Rigid slabs on a rigid deck

The square and triangular symbols in Figure 5 show transmissibilities calculated for the 1DOF and 2DOF lumped mass models.

For frequencies below the 12.5 Hz one-third octave band the transmissibilities differ by less than one decibel. The amplification in the 12.5 Hz one-third octave band is 16 dB. The 37.8 Hz mode of the 2DOF model increases the transmissibility by 15 dB compared to the 1DOF model in the 40 Hz one-third octave band.

At higher frequencies the 1DOF and 2DOF transmissibilities roll off with approximately 2 dB and 4 dB per one-third octave, respectively. This effect is due to the anti-phase condition[1] between m_1 and m_2 in the 2DOF model at frequencies above 37.8 Hz.

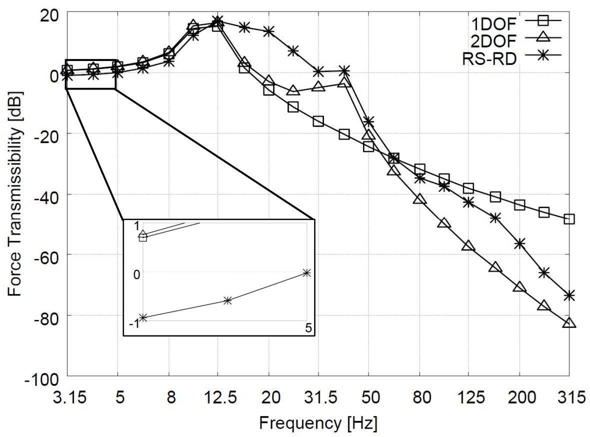

Figure 5. Calculated transmissibilities for the 1DOF and 2DOF models and the RS-RF model.

[1] The Eigenvectors normalized with respect to the displacement of m_1 are $(x_1;x_2)=(1; 1.149)$ and $(x_1;x_2)=(1; -2.521)$ for 11.5 Hz and 37.8 Hz, respectively.

The stars in Figure 5 show the transmissibility as calculated with the RS-RD FE model.

The RS-RD model yields negative transmissibilities for frequencies below the fundamental frequency. The transmissibility in the 3.15 Hz one-third octave band is –0.9 dB. This effect increases with increasing rail support flexibility and decreasing frequency.

In between the 12.5 Hz and 31.5 Hz band the transmissibility of the RS-RF FE model is significantly greater (>16 dB) than predicted by the two lumped mass models. This is due to a series of torsional rigid body modes of the slabs between 17 Hz and 28 Hz (Figure 9, Appendix A).

The results show that the transmissibility of the RS-RD model is greater than the 2DOF transmissibility in all one-third octave bands above the FST fundamental (i.e. the 2DOF model overestimates the vibration isolation performance compared to the RS-RD model).

This is primarily attributed to the high modal density of rail modes which are not accounted for in the 2DOF model. For example, the FE model exhibits four distinct unsprung mass modes in the 40 Hz one-third octave band compared to only one mode in the 2DOF model. In addition, differences in the implementation of the calculation of damping forces in the FE analysis compared to the analytical models start to gain weight with increasing frequency.

The results suggest that increasing the rail fastener stiffness will shift the rail resonance to higher frequencies, i.e. to the right. In general this results in an (unwanted) increase in force transmissibility. For the studied system, shifting the rail resonance towards higher frequencies result in a 4 dB increase per one-third octave band. The actual reduction in isolation performance, however, may be greater depending on the rail vibration spectrum.

Influence of flexibility

Flexibility of the slabs

The first bending mode of the studied floating slab is 220.8 Hz (Figure 10, Appendix A) and the first torsional mode is 262 Hz (Figure 11, Appendix A).

The stars in Figure 6 show the transmissibility as calculated with the RS-RF FE model. The circles show the influence of slab flexibility. It is evident that the assumption of rigid slabs is valid up to 160 Hz. Flexibility of the slabs increases the transmissibility by 3 dB, 13 dB and 10 dB in the 200 Hz, 250 Hz and 315 Hz one-third octave bands, respectively.

The predictions underestimate the increase in transmissibilities as the analysis is based on 5% critical damping but the slab modes are more lightly damped. This indicates serious degradation in isolation due to slab resonances. Shifting slab resonance to frequencies well above the typical frequency range of structure borne noise from track with resilient fasteners was an important design feature of the investigated double-tie FST (Ref. [4]).

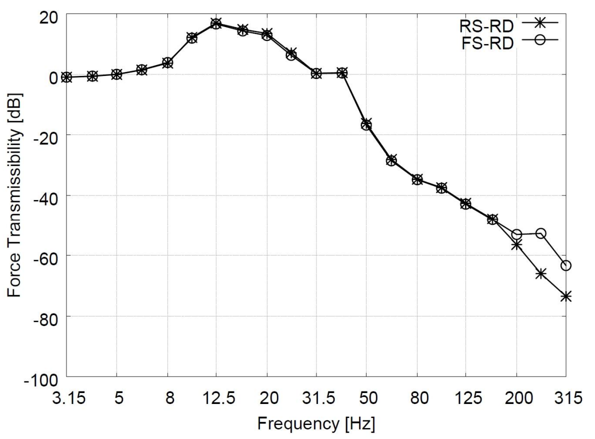

Figure 6. Calculated transmissibilities for rigid slabs and flexible slabs on a rigid deck.

Flexibility of the deck

The effects of two different deck supports were analysed. For the RS-FD(pS) case the fundamental deck resonance is calculated to be 30.2 Hz (Figure 12, Appendix A) and for the RS-FD(fC) case the fundamental deck resonance is calculated to be 18.7 Hz (Figure 13, Appendix A).

Calculated transmissibilities for the two considered flexible deck scenarios (triangular and square symbols) and the rigid deck results (star symbols) are presented in Figure 7.

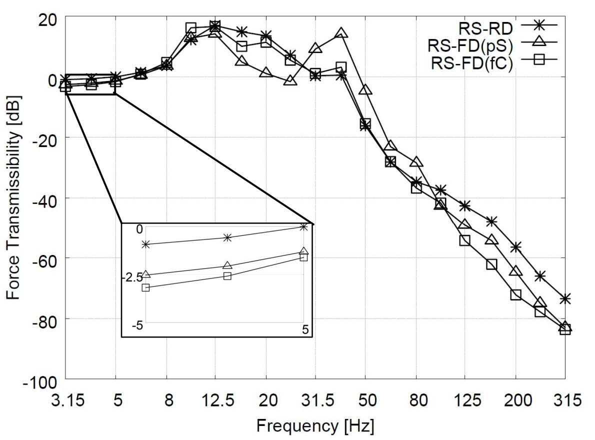

Figure 7. Calculated transmissibilities for rigid slabs on rigid and flexible decks.

Negative transmissibilities at low frequencies were discussed in the preceeding section and for a rigid support (RS-RD) the 3.15 Hz one-third octave band transmissibility was −0.9 dB. For the RS-FD(pS) and RS-FD(fC) support assumptions this results in a further reduction to −2.5 dB and −3.2 dB in the 3.15 Hz, respectively.

Comparing the RS-FD(pS) against the RS-RD results shows that a pronounced reduction in transmissibility of 8 dB to 12 dB is evident in the 16 Hz to 25 Hz one-third octave bands. This is driven by the torsional modes of the FST which fall into this frequency range and the fact that the four deck support points are directly under the centre line of the FST and, since they are pinned, they do not resist rotation of the deck (i.e. a nodal line (Figure 8)).

This shows that the force transmissibility can be influenced by positioning the support points. The decrease in force transmissibility also highlights that an analysis based on transmissibilities alone is not sufficient. Deck vibration levels must also studied.

The 30 Hz RS-FD(pS) deck resonance is driving the 9 dB and 14 dB transmissibility increase in the 31.5 Hz and 40 Hz one-third octave band.

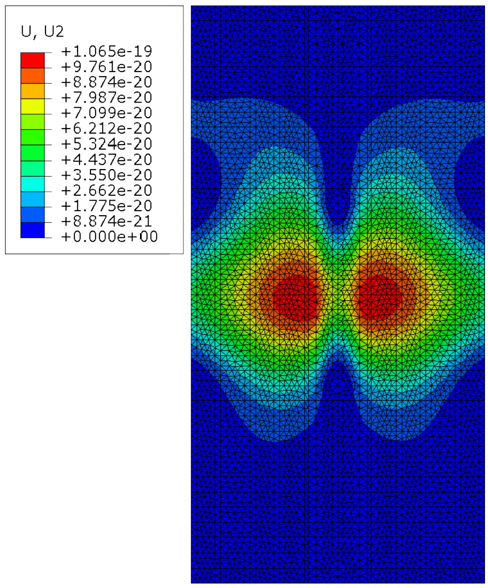

Figure 8. Calculated displacement PSD of the deck in vertical direction at 20 Hz (RS-FD(pS)).

Supporting the FST on a flexible deck and flexible columns (RS-FD(fC)) reduces the fundamental frequency from 11.5 Hz to 11.2 Hz and increases the transmissibility in the 10 Hz band.

The 18.7 Hz RS-FD(fC) deck resonance increases the transmissibility in the 16 Hz to 25 Hz one-third octave bands by 10 dB compared to the RS-FD(pS) scenario.

The results indicate that support flexibility reduces the transmissibilities at frequencies well above the fundamental deck modes. The rigid deck transmissibilities (RS-RD) are greater than the two considered flexible support transmissiblities in the 100 Hz one-third octave band and higher. In the 200 Hz one-third octave band the RS-RD transmissibility is 15 dB greater than the RS-FD(fC) transmissibility.

CONCLUSIONS

The force transmissibility of a double-tie FST installation was studied. Results from simple one and two degree of freedom lumped mass models were discussed and compared against FE models of varying complexity. The FE models were specifically used to study the influence of flexibility on the force transmissibility.

It was found that slab flexibility and flexibility of the FST support structure severely degade the vibration isolation performance at frequencies close to the corresponding fundamental frequencies of these elements. However, for the case of a flexible FST support structure the results indicate that flexibility can help to further reduce the vibration transmissibility at frequencies well above the fundamental frequency of the support structure.

The results also show that a design based on force transmissibility alone is not sufficient and that the deck response needs to be considered as well.

REFERENCES

1 P. H. Wirsching, T.L. Paez, K. Ortiz, *Random Vibrations - Theory and Practice* (Dover Publications, 2006)
2 C. W. de Silva, *Vibration and Shock Handbook* (CRC Press, 2005)
3 D. Duschlbauer, M. Pettersson, G. Lucas, J. Nelson, "Experimental and numerical analyses of a floating slab track" *Proceedings of ACOUSTICS* (2008), Geelong, Australia.
4 J. T. Nelson, M. Harrison, M. Pettersson, "Structure-borne Noise and Vibration Control for Chatswood Interchange" *Noise and Vibration Mitigation, NNFM99*, 143-149 (2008).
5 D. Thompson, *Railway Noise and Vibration* (Elsevier, 2009)
6 G. P. Wilson, "Rail System Noise and Vibration Control" *Proceedings of ACOUSTICS* (2004), Gold Coast, Australia
7 Abaqus 6.9, Dassault Systèmes Simulia Corp., Providence, RI, USA (2009)
8 K.A. Burgemeister, R.J. Greer, "Using Insertion Gains to Evaluate Railway Vibration Isolation Systems" *Proceedings of ACOUSTICS* (2004), Gold Coast, Australia

APPENDIX A – SELECTED MODESHAPES

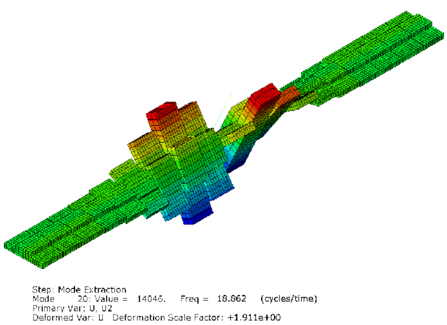

Figure 9. 18.9 Hz torsional FST mode (RS-RD).

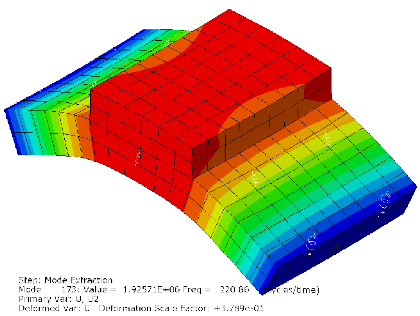

Figure 10. 221 Hz slab bending mode (FS-RD).

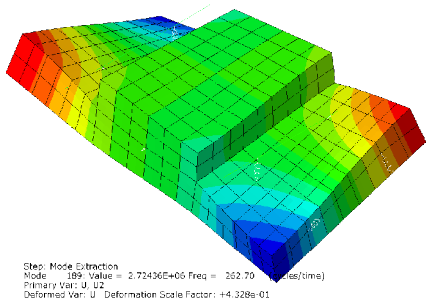

Figure 11. 263 Hz slab torsional mode (FS-RD).

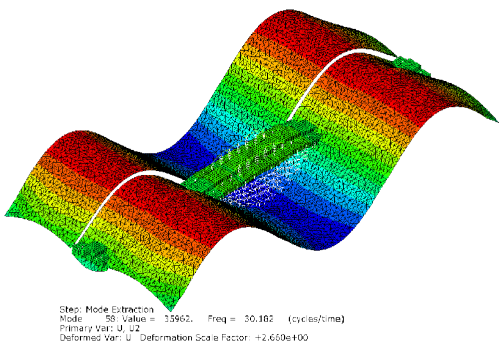

Figure 12. 30.2 Hz fundamental deck mode (RS-FD(pS)).

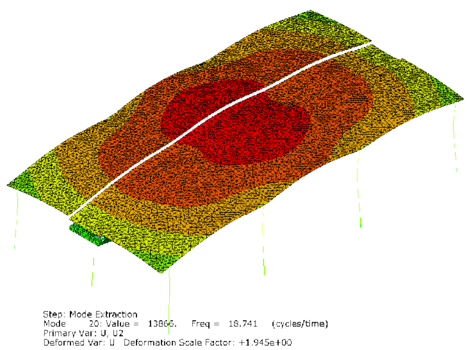

Figure 13. 18.7 Hz fundamental deck mode (RS-FD(fC)).